

Regulation of *OsSPL14* by *OsmiR156* defines ideal plant architecture in rice

Yongqing Jiao^{1,4}, Yonghong Wang^{1,4}, Dawei Xue²⁻⁴, Jing Wang¹, Meixian Yan², Guifu Liu¹, Guojun Dong², Dali Zeng², Zefu Lu¹, Xudong Zhu², Qian Qian² & Jiayang Li¹

Increasing crop yield is a major challenge for modern agriculture. The development of new plant types, which is known as ideal plant architecture (IPA), has been proposed as a means to enhance rice yield potential over that of existing high-yield varieties^{1,2}. Here, we report the cloning and characterization of a semidominant quantitative trait locus, *IPA1* (Ideal Plant Architecture 1), which profoundly changes rice plant architecture and substantially enhances rice grain yield. The *IPA1* quantitative trait locus encodes *OsSPL14* (SQUAMOSA PROMOTER BINDING PROTEIN-LIKE 14) and is regulated by microRNA (miRNA) *OsmiR156* *in vivo*. We demonstrate that a point mutation in *OsSPL14* perturbs *OsmiR156*-directed regulation of *OsSPL14*, generating an 'ideal' rice plant with a reduced tiller number, increased lodging resistance and enhanced grain yield. Our study suggests that *OsSPL14* may help improve rice grain yield by facilitating the breeding of new elite rice varieties.

Rice plant architecture is crucial for grain yield and is determined by plant height, tiller number and angle, and panicle morphology. The important characteristics of the ideal plant architecture (IPA) include low tiller numbers with few unproductive tillers, more grains per panicle than the currently cultivated varieties, and thick and sturdy stems^{1,2}. However, the molecular mechanisms for generating the IPA and increasing yield potential remain to be elucidated, and genes applicable for improving rice plant architecture are very limited. Different rice varieties have distinct plant architecture and therefore distinct yield potential. In comparison to currently cultivated rice varieties, including the *indica* variety Taichung Native 1 (TN1), the *japonica* line Shaoniejing (SNJ) has plant architecture that exemplifies the concept of IPA, including plant height, tiller number and panicle morphology (Fig. 1a). Backcrossing SNJ with TN1 or Hui7 (a *japonica* line) shows that plant height, tiller number and panicle morphology do not segregate in the backcross progenies, implying that the differences in plant architecture between TN1 or Hui7 and SNJ may be controlled by a single locus. We therefore designated the locus that determines the SNJ architecture as *IPA1*. Genetic analysis indicated that *IPA1* was semidominant, given that the phenotype of

heterozygous plants (*OsSPL14*^{IPA1/ipa1}) was intermediate between those of the homozygous plants *OsSPL14*^{IPA1/IPA1} and *OsSPL14*^{ipa1/ipa1} (Supplementary Fig. 1).

For the convenience of scoring the phenotype, we chose tiller number as the trait to use in mapping the *IPA1* locus. Using 110 BC₂F₂ plant lines generated from the backcross between SNJ and TN1, we detected the largest-effect quantitative trait locus (QTL), which explained 29.9% of tiller number variance, at *qTn8*. *qTn8* was mapped to the long arm of chromosome 8 between markers RM149 and RM1345 (Fig. 1b,c), which is most likely the same locus as that of a previously reported QTL that defines rice tiller number^{3,4}. To clone the gene underlying the *IPA1* locus, 5,500 BC₂F₂ plants that had similar tiller numbers to TN1 were identified and genotyped with newly developed molecular markers (Supplementary Table 1).

We narrowed the candidate region containing the *IPA1* locus to ~78 kb between markers M4 and M5 (Fig. 1d), which contains 12 predicted genes or ORFs (Fig. 1e and Supplementary Table 2; see URLs). Sequencing of the 12 genes in SNJ showed only one point mutation in the third exon of *OsSPL14* (LOC_Os08g39890; RAP ID Os08g0509600) compared to the Nipponbare variety of rice. This nucleotide substitution leads to an amino acid change from leucine to isoleucine in SNJ plants (Fig. 1f and Supplementary Fig. 2). In addition, Ri22, a *japonica* line showing similar plant architecture to SNJ, was also found to harbor an identical mutation in *OsSPL14*, whereas no mutation at this locus could be detected in the rice varieties TN1, 93-11 or Zhonghua11. We found that the expression level of *OsSPL14* was affected by the point mutation (Supplementary Fig. 3).

To determine whether *OsSPL14* underlies the *IPA1* QTL, we performed a confirmation test by generating transgenic plants expressing different levels of *OsSPL14* in the Nipponbare and Ri22 lines, the *japonica* varieties suitable for gene transformation. We introduced the plasmid carrying *OsSPL14* (designated *gOsSPL14*), which contained a 7.2-kb genomic DNA fragment, into Nipponbare (see Online Methods). The *gOsSPL14* transgenic lines had reduced tillers, stronger culms and increased panicle branches and grain yield (Supplementary Fig. 4). In contrast, the *OsSPL14* RNA interference (RNAi) transgenic plants in the Ri22 background generated more tillers and showed a marked reduction in plant height, diameter of culms, panicle branches

¹State Key Laboratory of Plant Genomics and National Center for Plant Gene Research, Institute of Genetics and Developmental Biology, Chinese Academy of Sciences, Beijing, China. ²State Key Laboratory of Rice Biology, China National Rice Research Institute, Chinese Academy of Agricultural Sciences, Hangzhou, China. ³Present address: College of Life and Environment Sciences, Hangzhou Normal University, Hangzhou, China. ⁴These authors contributed equally to this work. Correspondence should be addressed to J.L. (jyli@genetics.ac.cn) or Q.Q. (qianqian188@hotmail.com).

Received 11 February; accepted 21 April; published online 23 May 2010; doi:10.1038/ng.591

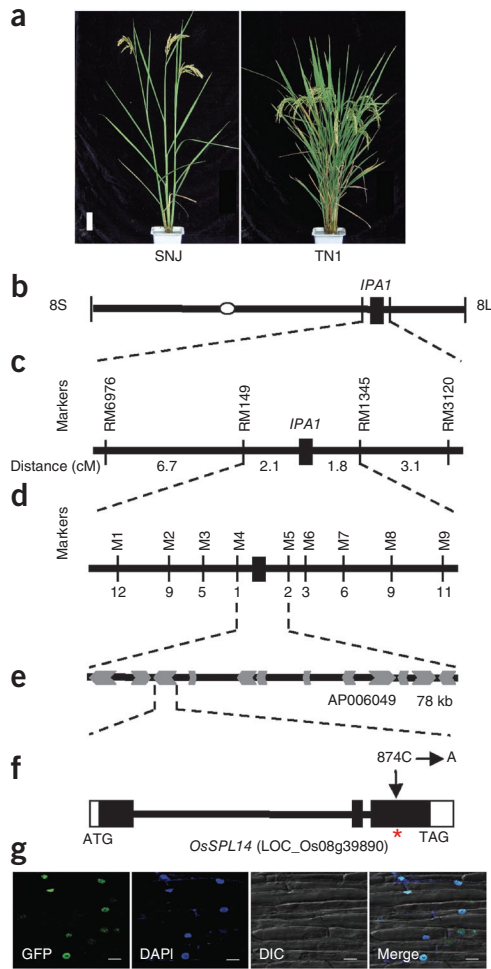


Figure 1 Map-based cloning of the *IPA1* QTL and subcellular localization of the *OsSPL14*-GFP fusion protein. (a) The plant architecture of SNJ and TN1. Scale bars, 10 cm. (b) Location of *IPA1* on rice chromosome 8. (c) Coarse linkage map of *IPA1*. (d) High-resolution linkage map of *IPA1*. The number of recombinants between the molecular marker and *IPA1* is indicated. (e) Annotation of the candidate region surrounding *IPA1* on BAC AP006049. Arrows indicate the putative genes predicted in the Rice Genome Annotation Database. (f) *OsSPL14* structure and the mutation site in SNJ. The white boxes represent the 5' and 3' untranslated regions, the black boxes represent the coding sequences and lines between boxes represent introns. The red asterisk indicates the *OsmiR156* target site. (g) Subcellular localization of *OsSPL14*-GFP in rice root cells. Scale bars, 10 μ m.

expressed in the shoot apex at both the vegetative (**Fig. 2a**) and reproductive (**Fig. 2b**) stages. It was also highly expressed in the promordia of primary and secondary branches (**Fig. 2c**).

Previous studies suggested that 11 *OsSPL* genes were putative targets of *OsmiR156* (ref. 8), a member of an miRNA family consisting of 19–25-base-pair noncoding single-stranded regulatory RNAs¹⁹. Bioinformatic analysis indicated that *OsSPL14* has the *OsmiR156* complementary site in the coding region (**Supplementary Fig. 2**). To determine whether *OsSPL14* could be regulated by *OsmiR156* *in vivo*, we mapped the *OsmiR156*-directed cleavage sites of *OsSPL14* by using RNA ligase-mediated rapid amplification of cDNA ends (RLM-RACE). Sequencing of 14 randomly chosen clones showed that 13 clones had 5' ends of the cleaved fragments in the middle region of the *OsmiR156* target site, indicating that *OsSPL14* can be precisely cleaved by *OsmiR156* *in vivo* (**Fig. 2d**).

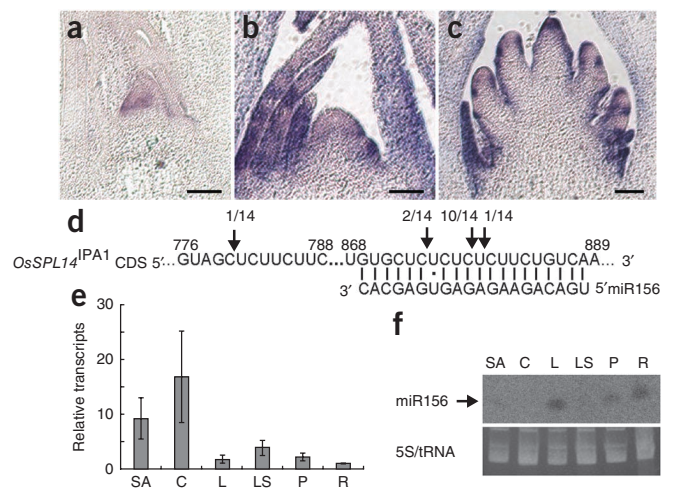
Expression patterns of *OsSPL14* and *OsmiR156* in various rice organs revealed by real-time PCR and miRNA gel blot analyses showed that *OsSPL14* was highly expressed in the culm and shoot apex, which is complementary with the expression pattern of *OsmiR156* *in vivo* (**Fig. 2e,f**). Consistently, overexpression of *OsmiR156* resulted in a substantial decrease in *OsSPL14* transcripts (**Supplementary Fig. 7a**), whereas the interruption of *OsmiR156* (overexpression of *MIM156*)²⁰ led to a marked increase in *OsSPL14* transcripts (**Supplementary Fig. 7b**). These results indicated that *OsSPL14* was regulated by the *OsmiR156*-directed cleavage *in vivo*.

MicroRNAs play important roles in modulating their target genes mainly through transcript cleavage in plants and mainly through translation repression in animals^{19,21,22}. Recent studies also showed that the translation inhibition of targets by miRNA was widespread in higher plants²³. To determine the molecular mechanism by which *OsSPL14* is regulated by *OsmiR156* *in vivo*, we sequenced the RT-PCR

and grain number (**Supplementary Fig. 5**). Therefore, we concluded that *OsSPL14* is the gene responsible for ideal plant architecture.

SPL genes, which share a highly conserved DNA-binding domain (the SBP domain), represent a family of plant-specific transcription factors that are involved in the regulation of flowering time, phase change, leaf initiation and other developmental processes in higher plants^{5–18}. In the rice genome, there are 19 *SPL* genes and *OsSPL14* (also known as *IPA1* and *WFP*) is most similar to *Arabidopsis SPL9* (ref. 8) (**Supplementary Fig. 6**), which has been suggested to be involved in regulating plastochron length and leaf size^{15,18}. *OsSPL14* is localized to the nucleus (**Fig. 1g**), consistent with a role as a transcription factor. RNA *in situ* hybridization revealed that *OsSPL14* was predominantly

Figure 2 Expression pattern of *OsSPL14* and confirmation of *OsmiR156*-directed regulation on *OsSPL14*. (a–c) *OsSPL14* expression patterns revealed by mRNA *in situ* hybridization. Scale bars, 200 μ m. (d) *OsmiR156* cleavage sites in *OsSPL14* mRNAs determined by RNA ligase-mediated 5' RACE. The vertical lines represent the nucleotides that base-pair with *OsmiR156* and dots show the mismatched nucleotide. The numbers above the sequence indicate the location of the nucleotide in the *OsSPL14* coding sequence. The positions corresponding to the 5' ends of the cleaved *OsSPL14* mRNAs determined by 5' RACE and the frequency of 5' RACE clones corresponding to each site are indicated by arrows. (e) *IPA1* transcript levels in various organs, including shoot apices of seedlings (SA), culms (C), leaves (L), leaf sheaths (LS), panicles after heading (P) and seedling roots (R). Values in e are means and s.d. of three independent experiments. (f) Expression pattern of *OsmiR156*. *OsmiR156* transcript levels were determined by RNA blot analysis in various organs.



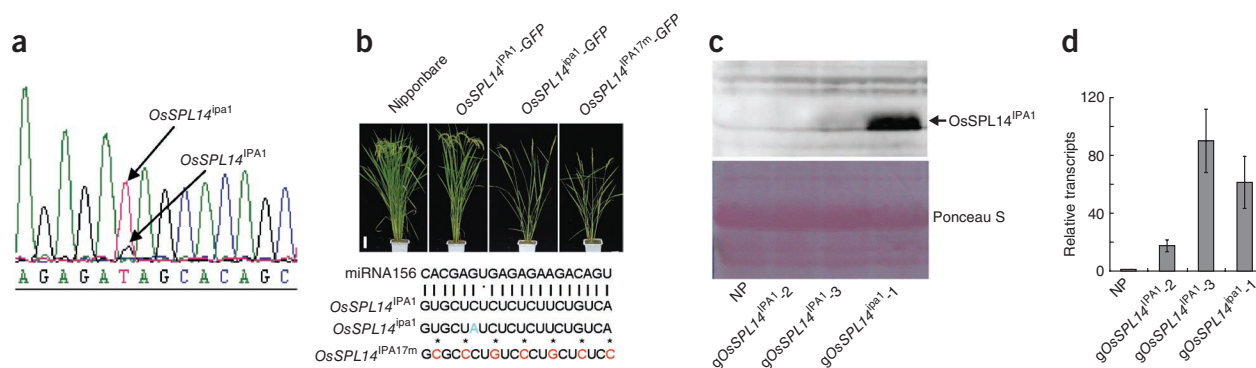


Figure 3 Effects of the point mutation in *OsSPL14*^{ipa1} on the OsmiR156-directed regulation of *OsSPL14*. **(a)** Chromatogram of intact *OsSPL14*^{IPA1/ipa1} mRNAs recovered from RT-PCR with primers flanking the cleavage site. Arrows indicate the different nucleotides in *OsSPL14*^{IPA1} and *OsSPL14*^{ipa1} cDNAs. **(b)** Phenotypes of *OsSPL14*^{IPA1-GFP}, *OsSPL14*^{ipa1-GFP} and *OsSPL14*^{IPA17m-GFP} transgenic plants. Scale bar, 10 cm. The blue letter indicates the mutation site in the *OsSPL14*^{ipa1} mRNA. The asterisks and red letters indicate the mutation sites and mutant nucleotides introduced into the OsmiR156 target site in the *OsSPL14*^{IPA17m-GFP} transgene, which interrupts the OsmiR156 target site without changing the amino acid residues. **(c)** Protein levels of IPA1 in Nipponbare (NP), *gOsSPL14*^{IPA1-2}, *gOsSPL14*^{IPA1-3} and *gOsSPL14*^{ipa1-1} transgenic plants. Above, protein blot with the antibody to IPA1; below, Ponceau S staining showing equal loading of proteins. **(d)** Transcript levels of *IPA1* revealed by real-time PCR in Nipponbare (NP), *gOsSPL14*^{IPA1-2}, *gOsSPL14*^{IPA1-3} and *gOsSPL14*^{ipa1-1} transgenic plants. Values are means and s.d. of three independent experiments.

products encompassing the cleavage site using the heterozygous (*OsSPL14*^{IPA1/ipa1}) plants and found that the intact mRNAs existed mainly as the *OsSPL14*^{ipa1} form (Fig. 3a). To confirm this, we further sequenced 37 clones from the RT-PCR products and found that 33 clones had the *OsSPL14*^{ipa1} form. These results suggest that the point mutation of *OsSPL14* in SNJ perturbed the cleavage of the *OsSPL14* transcripts by OsmiR156.

We generated transgenic plants carrying the *OsSPL14*^{IPA17m-GFP} transgene, which contained seven mismatches to OsmiR156 but did not introduce any amino acid changes (Fig. 3b). The phenotype of *OsSPL14*^{IPA17m-GFP} transgenic plants was very similar to those of *OsSPL14*^{ipa1-GFP} plants, and both of them had more severe phenotypes than the *OsSPL14*^{IPA1-GFP} transgenic plants (Fig. 3b), indicating that perturbing the OsmiR156 cleavage of *OsSPL14* even without changing the resulting amino acid sequence leads to alteration of the

plant architecture in SNJ. To investigate whether the point mutation perturbed the miRNA-directed translation repression of *OsSPL14*, we measured *OsSPL14* protein levels in transgenic plants with the plasmids *OsSPL14*^{ipa1} (*gOsSPL14*^{ipa1}) and *OsSPL14*^{IPA1} (*gOsSPL14*^{IPA1}). We found that *gOsSPL14*^{ipa1-1} transgenic plants had a significantly increased protein level as compared to both *gOsSPL14*^{IPA1-2} and *gOsSPL14*^{IPA1-3} plants, although the mRNA level in *gOsSPL14*^{ipa1-1} plants was lower than that in *gOsSPL14*^{IPA1-3} (Fig. 3c,d), suggesting that the point mutation may also perturb the OsmiR156-directed translation repression of *OsSPL14*. Therefore, the point mutation in the OsmiR156-complementary site of *OsSPL14* perturbs the OsmiR156-directed transcriptional cleavage and translation repression in rice.

To evaluate the application potential of *OsSPL14* for optimizing rice plant architecture and eventually improving grain yields, we generated a near-isogenic line (NIL) in the Hui7 genetic background that

Figure 4 Phenotypic characterization of NIL *OsSPL14*^{ipa1} plants. **(a)** Gross morphologies of NIL *OsSPL14*^{IPA1} and NIL *OsSPL14*^{ipa1} plants at maturity. Scale bar, 10 cm. **(b)** Panicles of NIL *OsSPL14*^{IPA1} and NIL *OsSPL14*^{ipa1}. Scale bar, 10 cm. **(c)** Culms of NIL *OsSPL14*^{IPA1} and NIL *OsSPL14*^{ipa1}. Scale bar, 5 cm. **(d)** Cross-sections of culms of NIL *OsSPL14*^{IPA1} and NIL *OsSPL14*^{ipa1} plants. The middle and right panels are magnifications of indicated square and circle regions in the left panel, respectively. BV, big vascular bundles; SV, small vascular bundles; SC, sclerenchyma cells. Bars, 100 μ m. **(e)** Comparison of the maximum bending force on third internodes between NIL *OsSPL14*^{IPA1} and NIL *OsSPL14*^{ipa1}. **(f)** Comparison of primary branch number per main panicle between NIL *OsSPL14*^{IPA1} and NIL *OsSPL14*^{ipa1}. **(g)** Comparison of secondary branch number per main panicle between NIL *OsSPL14*^{IPA1} and NIL *OsSPL14*^{ipa1}. **(h)** Comparison of grain number per main panicle between NIL *OsSPL14*^{IPA1} and NIL *OsSPL14*^{ipa1}. **(i)** Comparison of 1,000-grain weight between NIL *OsSPL14*^{IPA1} and NIL *OsSPL14*^{ipa1}. **(j)** Comparison of the grain yield per main panicle between NIL *OsSPL14*^{IPA1} and NIL *OsSPL14*^{ipa1}. Values in e–j are means \pm s.d. (e–h, $n = 12$ plants; i, $n = 3$ replicates). The double asterisks represent significance difference determined by the Student's *t*-test at $P < 0.01$.

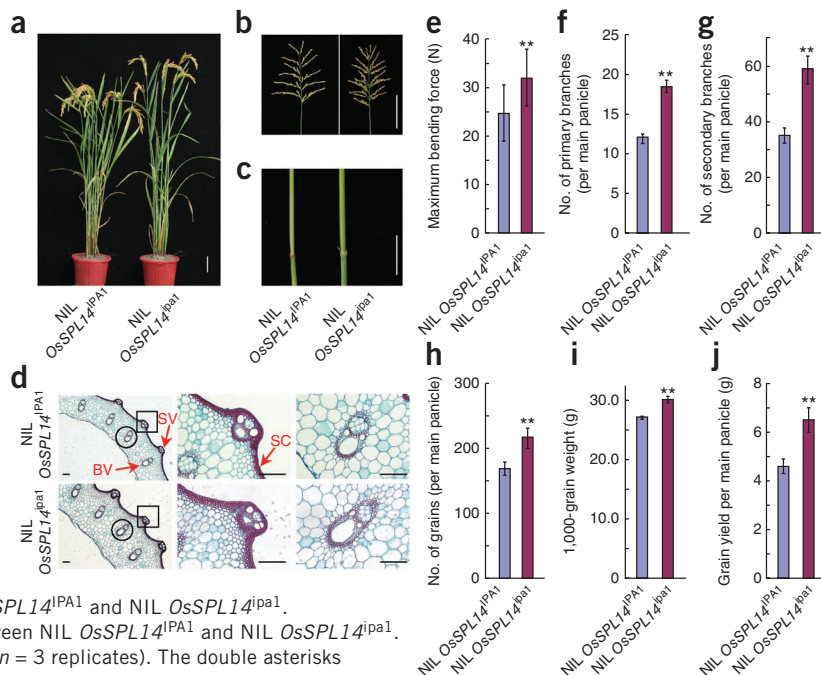


Table 1 Yield test in a paddy between XS11 and NIL XS11 *OsSPL14*^{ipa1} plants

Traits	XS11	XS11 <i>OsSPL14</i> ^{ipa1}
Panicles per plot	1,972.7 ± 39.1	1,079.3 ± 22.2
Grains per panicle	91.8 ± 3.2	173.2 ± 7.5
1,000-grain weight (g)	27.5 ± 0.2	29.6 ± 0.5
Theoretical yield per plot (kg)	4.98 ± 0.10	5.53 ± 0.11
Theoretical yield increase over XS11 (%)	–	11.1
Actual yield per plot (kg)	4.44 ± 0.12	4.92 ± 0.14
Actual yield increase over XS11 (%)	–	10.7

Data are from plants in randomized complete block design with three replications under natural condition in Hangzhou, China, in 2008. The planting density was 19.98 cm × 23.31 cm, with one plant per hill. The area per plot was 6.67 m². Values are means ± s.d.

contains the *OsSPL14*^{ipa1} allele. The resulting NIL *OsSPL14*^{ipa1} plant showed an increase in accumulation of the *OsSPL14* transcript and protein in comparison with NIL *OsSPL14*^{IPA1} plants (Supplementary Fig. 8). Compared with the NIL *OsSPL14*^{IPA1} plant, the NIL *OsSPL14*^{ipa1} plant is taller (Fig. 4a and Supplementary Fig. 9a) and has fewer tillers (Fig. 4a and Supplementary Fig. 9b), denser panicles (Fig. 4b) and stronger culms (Fig. 4c and Supplementary Fig. 9c). In-depth characterization of these traits revealed that the reduced tiller number in NIL *OsSPL14*^{ipa1} plants resulted from the prolonged plastochron (Supplementary Fig. 10a). The cross-section of the culm internodes showed that the NIL *OsSPL14*^{ipa1} plant had more vascular bundles and sclerenchyma cells than the NIL *OsSPL14*^{IPA1} plant (Fig. 4d and Supplementary Fig. 10b). Consistently, the culm mechanical strength of the NIL *OsSPL14*^{ipa1} plant was significantly increased in comparison with NIL *OsSPL14*^{IPA1} plants (Fig. 4e). More importantly, statistical analysis indicated that the NIL *OsSPL14*^{ipa1} panicle produced more primary and secondary branches (Fig. 4f,g) and more grains (Fig. 4h). Thousand-grain weight increased from 27.2 g in NIL *OsSPL14*^{IPA1} to 30.2 g in NIL *OsSPL14*^{ipa1} (Fig. 4i). Theoretically, the grain yield of NIL *OsSPL14*^{ipa1} panicles showed an increase of 6.5 g per main panicle compared to 4.6 g per main panicle in NIL *OsSPL14*^{IPA1} (Fig. 4j). Introduction of the *OsSPL14*^{ipa1} allele into Xiushui 11 (XS11), a japonica rice variety cultivated in South China, increased the grain yield by ~10% in the test plot (Table 1). These results indicate that *OsSPL14* is a pleiotropic gene that appears to confer an ideal rice plant architecture with few unproductive tillers, enhanced grain yield per panicle and an elevated lodging resistance. Taken together, our findings show that *OsSPL14* is an important semidominant regulator of rice plant architecture. *OsSPL14* may help facilitate the genetic engineering and molecular breeding of elite rice varieties with ideal plant architecture to reach much higher yield potential.

URLs. <http://rice.plantbiology.msu.edu/cgi-bin/gbrowse/rice/>.

METHODS

Methods and any associated references are available in the online version of the paper at <http://www.nature.com/naturegenetics/>.

Accession codes. *IPA1* is deposited in GenBank under the following number: GU136674.

Note: Supplementary information is available on the Nature Genetics website.

ACKNOWLEDGMENTS

We thank K. Chong (Institute of Botany, Chinese Academy of Sciences) for providing the pTCK303 vector. This work was supported by grants from Ministry of Agriculture of the People's Republic of China (2008ZX08009), Ministry of Science and Technology (2005CB1208) and National Natural Science Foundation of China (30710103903).

AUTHOR CONTRIBUTIONS

Y.J. and Y.W. designed the research, performed experiments, analyzed data and wrote the paper. D.X. performed experiments and analyzed data. J.W., M.Y., G.L., G.D., D.Z., Z.L. and X.Z. performed the experiments. Q.Q. designed the research and analyzed the data. J.L. supervised the project, designed research, analyzed data and wrote the paper.

COMPETING FINANCIAL INTERESTS

The authors declare no competing financial interests.

Published online at <http://www.nature.com/naturegenetics/>.

Reprints and permissions information is available online at <http://npg.nature.com/reprintsandpermissions/>.

1. Khush, G.S. Breaking the yield frontier of rice. *GeoJournal* **35**, 329–332 (1995).
2. Virk, P.S., Khush, G.S. & Peng, S. Breeding to enhance yield potential of rice at IRRI: the ideotype approach. *Int. Rice Res. Notes* **29**, S1–S9 (2004).
3. Miyamoto, N. *et al.* Quantitative trait loci for phyllochron and tillering in rice. *Theor. Appl. Genet.* **109**, 700–706 (2004).
4. Fukuta, Y. *et al.* Identification of low tiller gene in rice two varieties, Aikawa 1 and Shuho in rice (*Oryza sativa* L.). *Plant and Animal Genome XII Abstract*, 167 (2004).
5. Klein, J., Saedler, H. & Huijser, P. A new family of DNA binding proteins includes putative transcriptional regulators of the *Antirrhinum majus* floral meristem identity gene *SQUAMOSA*. *Mol. Gen. Genet.* **250**, 7–16 (1996).
6. Cardon, G. *et al.* Molecular characterisation of the *Arabidopsis* SBP-box genes. *Gene* **237**, 91–104 (1999).
7. Gandikota, M. *et al.* The miRNA156/157 recognition element in the 3' UTR of the *Arabidopsis* SBP box gene *SPL3* prevents early flowering by translational inhibition in seedlings. *Plant J.* **49**, 683–693 (2007).
8. Xie, K., Wu, C. & Xiong, L. Genomic organization, differential expression, and interaction of *SQUAMOSA* promoter-binding-like transcription factors and microRNA156 in rice. *Plant Physiol.* **142**, 280–293 (2006).
9. Unte, U.S. *et al.* *SPL8*, an SBP-box gene that affects pollen sac development in *Arabidopsis*. *Plant Cell* **15**, 1009–1019 (2003).
10. Stone, J.M., Liang, X., Nekl, E.R. & Stiers, J.J. *Arabidopsis AtSPL14*, a plant-specific SBP-domain transcription factor, participates in plant development and sensitivity to fumonisin B1. *Plant J.* **41**, 744–754 (2005).
11. Manning, K. *et al.* A naturally occurring epigenetic mutation in a gene encoding an SBP-box transcription factor inhibits tomato fruit ripening. *Nat. Genet.* **38**, 948–952 (2006).
12. Wu, G. & Poethig, R.S. Temporal regulation of shoot development in *Arabidopsis thaliana* by miR156 and its target *SPL3*. *Development* **133**, 3539–3547 (2006).
13. Zhang, Y., Schwarz, S., Saedler, H. & Huijser, P. *SPL8*, a local regulator in a subset of gibberellin-mediated developmental processes in *Arabidopsis*. *Plant Mol. Biol.* **63**, 429–439 (2007).
14. Lee, J., Park, J.J., Kim, S.L., Yim, J. & An, G. Mutations in the rice *liguleless* gene result in a complete loss of the auricle, ligule, and laminar joint. *Plant Mol. Biol.* **65**, 487–499 (2007).
15. Wang, J.W., Schwab, R., Czech, B., Mica, E. & Weigel, D. Dual effects of miR156-targeted *SPL* genes and *CYP78A5/KLUH* on plastochron length and organ size in *Arabidopsis thaliana*. *Plant Cell* **20**, 1231–1243 (2008).
16. Wu, G. *et al.* The sequential action of miR156 and miR172 regulates developmental timing in *Arabidopsis*. *Cell* **138**, 750–759 (2009).
17. Wang, J.W., Czech, B. & Weigel, D. miR156-regulated *SPL* transcription factors define an endogenous flowering pathway in *Arabidopsis thaliana*. *Cell* **138**, 738–749 (2009).
18. Schwarz, S., Grande, A.V., Bujdosó, N., Saedler, H. & Huijser, P. The microRNA regulated SBP-box genes *SPL9* and *SPL15* control shoot maturation in *Arabidopsis*. *Plant Mol. Biol.* **67**, 183–195 (2008).
19. Stefani, G. & Slack, F.J. Small non-coding RNAs in animal development. *Nat. Rev. Mol. Cell Biol.* **9**, 219–230 (2008).
20. Franco-Zorrilla, J.M. *et al.* Target mimicry provides a new mechanism for regulation of microRNA activity. *Nat. Genet.* **39**, 1033–1037 (2007).
21. Mallory, A.C. & Vaucheret, H. Functions of microRNAs and related small RNAs in plants. *Nat. Genet.* **38**Suppl, S31–S36 (2006).
22. Jones-Rhoades, M.W., Bartel, D.P. & Bartel, B. MicroRNAs and their regulatory roles in plants. *Annu. Rev. Plant Biol.* **57**, 19–53 (2006).
23. Brodersen, P. *et al.* Widespread translational inhibition by plant miRNAs and siRNAs. *Science* **320**, 1185–1190 (2008).

ONLINE METHODS

Plant materials. The *japonica* background SNJ and Ri22 carry the *OsSPL14*^{IPa1} allele and have similar plant architecture. The *japonica* line Hui7 and the *indica* variety TN1 have different plant architecture from SNJ and Ri22. Plants from the Hui7 × SNJ F₁ generation were backcrossed four times with Hui7 to generate the near-isogenic line Hui7 (NIL *OsSPL14*^{IPa1}). To breed an elite rice variety harboring the *OsSPL14*^{IPa1} allele, XS11 × SNJ F₁ plants were backcrossed three times with XS11 to generate the BC₃F₁ seeds. From the BC₃F₂ generation, the NIL XS11 *OsSPL14*^{IPa1} was developed for the yield test in this study.

Constructs for genetic transformation. To construct the g*OsSPL14*^{IPa1} transformation plasmid, a 7.2-kb DNA fragment containing a 1,117-bp upstream sequence, the entire *OsSPL14*^{IPa1} and a 2,326-bp downstream region was amplified from the Nipponbare genomic DNA using primers gIPA11F and gIPA11R (Supplementary Table 1), then digested with KpnI and XbaI and ligated to the binary vector pCAMBIA1300 for gene transformation. To construct the *OsSPL14* RNAi plasmid, two DNA fragments (610 base pairs long) were amplified from the full-length cDNA clone AK107191 using two pairs of primers RNAi1F and RNAi1R, and RNAi2F and RNAi2R (Supplementary Table 1). The BamHI-KpnI- and SacI-SpeI-digested fragments were cloned into the binary vector pTCK303²⁴. To construct the *OsSPL14*^{IPa1}-GFP plasmid, the PCR products containing the *OsSPL14*^{IPa1} promoter region and the entire *OsSPL14* coding sequence were amplified using primers gIPA11R and IPA1GFP2R (Supplementary Table 1) from the mixture of *OsSPL14* promoter-containing PCR products amplified with primers gIPA11R and IPA1GFP1R (Supplementary Table 1) and the *OsSPL14* coding sequence-containing PCR products with primers IPA1OE1F and IPA1GFP2R (Supplementary Table 1). The KpnI-XbaI-digested fragments were ligated into the binary vector AHLG. The mutations in *OsSPL14*^{IPa1}-GFP and *OsSPL14*^{IPa17m}-GFP were introduced by primers gipa11F, gipa11R and 7mIPA1GFP1F, 7mIPA1GFP1R (Supplementary Table 1). To construct the miRNA156OE plasmid, the PCR fragments amplified from the full length cDNA clone AK110797 using primers 156OE1F and 156OE1R (Supplementary Table 1) were subcloned into the BamHI-SacI-digested binary vector pTCK303. The MIM156 construct was generated according to previously reported method²⁵, and the PCR fragment was subcloned into the BamHI-SacI-digested pTCK303 vector.

5' modified rapid amplification of cDNA ends. 5' modified RACE was performed according to the method reported previously²⁶. Briefly, total RNA was isolated from 2-week-old NIL *OsSPL14*^{IPa1} seedlings using the TRIzol Reagent (Invitrogen). The gene specific primers of *OsSPL14* for the first and second PCR products are IPA1-1570R and IPA1RT1R (Supplementary Table 1), respectively. The second PCR products were gel purified and subcloned into the pGEM-T Easy Vector (Promega) for sequencing.

Antibody preparation. A DNA fragment encoding the *OsSPL14*^{IPa1} amino acid residues 1–96 amplified with the primers IPA1OE1F and IPA1P1R (Supplementary Table 1) was subcloned into pET28a. The recombinant *OsSPL14*^{IPa1} protein was expressed in BL21 cells, purified by Chelating Sepharose Fast Flow (GE Healthcare) according to the supplier's instructions and used to raise polyclonal antibodies in rabbits. The resulting *OsSPL14*^{IPa1} antibodies were purified through an IgG affinity chromatography column before use. The specificity of the antibody was determined by protein blot (Supplementary Fig. 11).

Determination of transcript levels of *OsSPL14* by real-time PCR and OsmiR156 with RNA blot. Total RNAs were prepared using a TRIzol kit according to the user's manual (Invitrogen). Total RNAs from various organs were split into two portions, one for the detection of *OsSPL14* by real-time PCR and one for OsmiR156 by RNA blot. For determination of *OsSPL14* transcripts, one microgram of total RNA was treated with DNase I and used for

cDNA synthesis with a reverse transcription kit (Promega). Real-time PCR experiments were performed using gene-specific primers in a total volume of 10 μl with 1 μl of the reverse transcriptase reactions, 1 μM of the gene-specific primers IPA1rttime1F and IPA1rttime1R (Supplementary Table 1) and 5 μl SYBR Green Master mix (Applied Biosystems) on an ABI 7900 real-time PCR machine (Applied Biosystems) according to the manufacturer's instructions. The rice *Ubiquitin* gene (Os03g0234200) was used as the internal control. The relative *OsSPL14* transcript levels in various organs were compared with that in the root, after normalization with *Ubiquitin* transcript and averaged from three independent replicates. For the detection of OsmiR156, 40 μg of total RNAs from various organs were resolved in 15% polyacrylamide-urea gels, electro-transferred to Zeta-Probe membranes (Bio-Rad) and hybridized to an antisense oligonucleotide probe (Supplementary Table 1).

Determination of *OsSPL14* transcripts and *OsSPL14*^{IPa1} protein abundance. Two-week-old seedlings were ground into fine powder in liquid nitrogen and divided into two parts, one for detecting of *OsSPL14*^{IPa1} transcripts and the other for measuring *OsSPL14*^{IPa1} protein abundance. For detecting *OsSPL14*^{IPa1} transcripts by RNA blot, 20 μg of total RNAs were separated on a 1.2% denaturing gel, transferred to nylon filters (Hybond-N⁺, Amersham) and hybridized to the *OsSPL14*-specific probe amplified from the full-length cDNA clone AK107191 using the primers RNAi1F and RNAi1R (Supplementary Table 1). For measuring the *OsSPL14*^{IPa1} protein abundance, total proteins were extracted using the extraction buffer (500 mM Tris-HCl, pH 7.5, 150 mM NaCl, 0.1% NP-40 detergent, 4 M urea, 1 mM PMSF inhibitor) and quantified by the Bio-Rad protein assay. Protein blot was performed with the SuperSignal West chemiluminescence kit according to the manufacturer's protocol (Pierce Chemical) using the *OsSPL14*^{IPa1} antibody.

Measurement of physical properties. The maximum bending force was measured using a digital force/length tester (5848 microtester, Istron; <http://www.istron.com/>). The third internodes of NIL *OsSPL14*^{IPa1} and NIL *OsSPL14*^{IPa1} plants were used for the measurement.

RNA *in situ* hybridization and subcellular localization of *OsSPL14*. RNA *in situ* hybridization was performed as described previously²⁷ with minor modification. Briefly, the 610-bp region of *OsSPL14* was subcloned into the pGEM-T Easy (Promega) vector and used as the template to generate sense and antisense RNA probes. Digoxigenin-labeled RNA probes were prepared using a DIG Northern Starter Kit (cat. no. 2039672, Roche) according to the manufacturer's instruction. Slides were observed under bright field through a microscope (Leica DMR) and photographed with a Micro Color charge-coupled device camera (Apogee Instruments).

To examine the subcellular localization of *OsSPL14*^{IPa1} in rice cells, the PCR fragment amplified from the full length cDNA clone AK107191 using the primers IPA1GFPACF and IPA1GFP2R (Supplementary Table 1) was ligated into the binary vector AHLG under the control of the rice *ACTIN* promoter. The recombinant plasmid was introduced into Nipponbare plants by *Agrobacterium tumefaciens*-mediated transformation. Transgenic seeds of the T₁ progeny were screened on agar plates containing 50 mg/l hygromycin. Fluorescence analysis was carried out on roots 5 d post germination. GFP signals were examined and photographed under a confocal microscope at an excitation wavelength of 488 nm (FluoView 1000; Olympus).

24. Wang, Z. *et al.* A practical vector for efficient knockdown of gene expression in rice (*Oryza sativa* L.). *Plant Mol. Biol. Rep.* **22**, 409–417 (2004).
25. Franco-Zorrilla, J.M. *et al.* Target mimicry provides a new mechanism for regulation of microRNA activity. *Nat. Genet.* **39**, 1033–1037 (2007).
26. Llave, C., Xie, Z., Kasschau, K.D. & Carrington, J.C. Cleavage of Scarecrow-like mRNA targets directed by a class of *Arabidopsis* miRNA. *Science* **297**, 2053–2056 (2002).
27. Li, P. *et al.* LAZY1 controls rice shoot gravitropism through regulating polar auxin transport. *Cell Res.* **17**, 402–410 (2007).